Weighted-density-functional theory calculation of elastic constants for face-centered-cubic and body-centered-cubic hard-sphere crystals

Brian B. Laird

Department of Chemistry, University of Utah, Salt Lake City, Utah 84112

The isothermal elastic constants for the face-centered-cubic (fcc) and body-centered-cubic (bcc) hard-sphere crystal are calculated for a range of densities using the modified weighted-density functional of Denton and Ashcroft [Phys. Rev. A **39**, 4701 (1989)]. The fcc elastic constants are shown to be in excellent agreement with the computer simulation data and to represent a significant improvement over the predictions of other density-functional methods. The bcc crystal is predicted correctly to be unstable to shear, in agreement with simulation. This fact supports the conclusion that the bcc hard-sphere solid, even though mechanically unstable, is well described by such methods.

I. INTRODUCTION

The calculation of the elastic constants of hard-sphere solids using various forms of density-functional theory has been the subject of several recent papers.[1-5] Such calculations are much more sensitive measures of the accuracy of a particular density-functional technique than the determination of the solid–liquid freezing point. Although varying in absolute accuracy relative to the computer-simulation results,[6] most proposed versions of density-functional theory give at least qualitatively reasonable results when applied to the hard-sphere (face-centered-cubic) solid to fluid transition,[7-14] whereas the results of calculations for the elastic constants involving the same set of theories differ dramatically. This sensitivity is expected because evaluation of elastic constants involves the determination of the second derivatives of the Helmholtz free energy, a procedure that tends to magnify the shortcomings of any theory.

Two early calculations[2-3] generated some controversy because they predicted a negative Poisson ratio for the hard-sphere face-centered-cubic fcc crystal. This result implies the somewhat counterintuitive situation that when a uniaxial compression is applied along one Cartesian direction, the crystal responds by *contracting* along the other two axes. Both of these calculations were based on a version[7,15] of density-functional theory in which the free energy of the inhomogeneous phase (solid) is given by a second-order expansion about a reference phase, in this case, the coexisting liquid. Later computer simulations[16,17] put the matter to rest by showing that this conclusion was false and the Poisson ratio was indeed positive at densities at which the crystal is thermodynamically stable.

Two later density-functional calculations gave more promising results. The first, by Velasco and Tarazona,[4] was based on an early version of weighted-density-functional theory. The second by Baus and Xu[11] used the so-called effective liquid approximation (ELA), which is similar in form to the earlier "second-order" theories, but the density of the fluid whose properties are used to construct the free-energy functional for the solid phase is chosen rather arbitrarily so that the position of the first peak in the fluid structure factor $S(k)$ corresponds to the first reciprocal lattice vector of the crystal under study. Both studies, which are designed to include higher-order terms in the functional expansion in an implicit and *ad hoc* manner, give qualitatively reasonable results for the fcc elastic constants.

Building on the work of Tarazona,[8] Curtin and Ashcroft[10] developed the so-called weighted-density approximation (WDA). In this theory, the free-energy functional is constructed in such a way that the first two functional derivatives with respect to the density yield the correct result in the homogeneous (liquid) limit. Because of these constraints, the WDA can be considered to have a firmer theoretical basis than earlier nonperturbative theories. Later, Denton and Ashcroft[13] developed a related, but simpler approach known as the modified weighted-density approximation (MWDA). The MWDA is easier to use than the WDA and, at least for freezing, provides the same level of accuracy. Based on its simplicity and good results for hard spheres and other systems, the MWDA is the most useful density-functional theory currently available.

In this paper, the MWDA is used to calculate the elastic constants for the fcc hard-sphere crystal. Given the previously mentioned sensitivity of the elastic constant on the density-functional method used, this should be a critical test of this theory. When compared to the simulation data, the results of this calculation are very good and are superior to those of previous calculations.

In addition to the fcc hard-sphere crystal, the elastic constants for the body-centered-cubic (bcc) crystal are also calculated. While it is well known that the bcc hard-sphere crystal is mechanically unstable to shear fluctuations, Curtin and Runge[18] have shown that the WDA gives reasonable free energies for the bcc hard-sphere solid if the free-energy minimization only includes uniform expansions or contractions of the lattice, thereby excluding *a priori* the shear distortions that would show the instability. This hard-sphere bcc phase, although unstable, is of interest because neither the WDA nor the MWDA give bcc solutions for systems such as the inverse sixth-power potential,[19] for which simulations[20] show that such a structure is both mechanically and thermodynamically stable along the freezing line. Given this failure of these (and all earlier) density-functional theories for non-close-packed crystals of relatively long-ranged po-

tentials, the hard-sphere bcc phase, if described correctly, could give a starting point for a possible perturbation approach.

As the elastic constants measure the curvature of the free-energy surface about a given structure, their calculation for the bcc hard-sphere crystal will show whether this phase is mechanically stable or unstable. Since it is known that this structure is unstable in reality, the correct prediction of this by the MWDA will indicate that this approach describes the free-energy surface at least qualitatively. To this end, it is promising that the present calculations of the bcc hard-sphere elastic constants show that the MWDA does predict correctly the instability of this crystal.

II. ELASTIC CONSTANTS

The elastic constants of a system measure the thermodynamic response of the system to an externally induced distortion that is both uniform and small. Such a distortion or "strain" can be represented by a linear point transformation

$$R_i = r_i^0 + u_{ij} r_j^0, \tag{1}$$

where $\mathbf{r}^0$ and $\mathbf{r}$ are the initial and post-distortion coordinate vectors, respectively, of any point in the system, and u_{ij} is called the displacement gradient.

The symmetric Lagrangian (or "finite") strain tensor η is defined as

$$n_{ij} = \tfrac{1}{2}(u_{ij} + u_{ji} + u_{ki} u_{kj}), \tag{2}$$

where here and in what follows, the Einstein summation convention, whereby repeated indices are summed over, is assumed. It can be shown readily that this strain tensor, so defined, governs the change, due to the distortion, in the distance between two arbitrary points in the system. Since the internal energy is dependent only on the relative positions of the particles that make up the system, any change in the thermodynamic state of the system can be described as a function of η alone. That η is a symmetric tensor ensures that it is invariant to any pure rotation.

Because the strain is assumed to be small, the Helmholtz free energy per unit volume can be expanded in a Taylor series about the undistorted state

$$\frac{\mathscr{F}(\eta)}{V} = \frac{\mathscr{F}(0)}{V} + T_{ij}^0 \eta_{ij} + \frac{1}{2} C_{ijkl} \eta_{ij} \eta_{kl} + \cdots, \tag{3}$$

where

$$T_{ij}^0 = \frac{1}{V}\left(\frac{\partial \mathscr{F}}{\partial \eta_{ij}}\right)_{\eta=0} \tag{4}$$

is the stress tensor for the undistorted system and

$$C_{ijkl} = \frac{1}{V}\left(\frac{\partial^2 \mathscr{F}}{\partial \eta_{ij} \partial \eta_{kl}}\right)_{\eta=0} \tag{5}$$

are the (isothermal) elastic constants. For a system whose initial stress corresponds to an isotropic pressure p,

$$T_{ij}^0 = -p\delta_{ij}. \tag{6}$$

Since the strain is assumed to be small, one is tempted to argue that the third term of the right-hand side of Eq. (2) can be ignored as it is of second order in the displacement gradient. One could then define an "infinitesimal" strain tensor

$$\epsilon_{ij} = \tfrac{1}{2}(u_{ij} + u_{ji}) \tag{7}$$

and a corresponding set of elastic constants

$$B_{ijkl} = \frac{1}{V}\left(\frac{\partial^2 \mathscr{F}}{\partial \epsilon_{ij} \partial_{kl}}\right)_{\epsilon=0}. \tag{8}$$

However, elastic constants so defined differ from C_{ijkl} defined in Eq. (6) by terms proportional to the initial stress tensor since the first-order term $T_{ij}^0 \eta_{ij}$ in Eq. (4) contains terms that are second order in ϵ that will also contribute to the B_{ijkl}'s. Only in the case of zero initial stress are the two definitions identical.

From the definitions given above, the following symmetries follow:

$$\eta_{ij} = n_{ji}, \tag{9}$$

$$T_{ij} = T_{ji}, \tag{10}$$

$$C_{ijkl} = C_{jikl} = C_{klij} = \cdots. \tag{11}$$

Using these index permutation symmetries, it is possible to decrease the number of indices of the elastic constants from four to two using the standard Voigt notation $11 \to 1$, $22 \to 2$, $33 \to 3$, 12, and $21 \to 5$, 23; and $32 \to 5$, 13 and $31 \to 6$ (e.g., $C_{1132} \to C_{15}$). For the cubic systems considered here, only 12 of the possible 36 Voigt elastic constants $C_{\alpha\beta}$ are nonzero and of these there are only three independent ones. C_{11}, C_{12}, and C_{44} can be taken to be a complete set.

Once a method is specified for determining the free energy of the cubic solid after a deformation transformation has been applied, the three independent elastic constants can be determined using the following procedure: First, three different displacement tensors [see Eq. (1)] are defined

$$u_{ij}^{(1)} = \epsilon_1 \delta_{ij}, \tag{12}$$

$$u_{ij}^{(2)} = \epsilon_2 \delta_{i1} \delta_{j1}, \tag{13}$$

$$u_{ij}^{(3)} = \epsilon_3 (\delta_{i1} \delta_{j2} + \delta_{i2} \delta_{j1}). \tag{14}$$

The desired elastic constants can then be determined in terms of derivatives of the free energy with respect to ϵ_1, ϵ_2, and ϵ_3,

$$\rho\frac{\partial \mathscr{F}}{\partial \epsilon_1} = -3P, \tag{15}$$

$$\rho\frac{\partial^2 \mathscr{F}}{\partial \epsilon_1^2} = 3(C_{11} + 2C_{12} - P), \tag{16}$$

$$\rho\frac{\partial^2 \mathscr{F}}{\partial \epsilon_2^2} = C_{11} - P, \tag{17}$$

$$\rho\frac{\partial^2 \mathscr{F}}{\partial \epsilon_3^2} = 2(2C_{44} - P). \tag{18}$$

The requirement of mechanical stability puts restrictions on the various elastic constants for a stable crystal. For a cubic system, these conditions can be shown[21] to be

$$C_{11} - P > 0, \tag{19}$$

$$C_{44} - P > 0, \tag{20}$$

$$C_1 \equiv \frac{C_{11} - C_{12}}{2} - P > 0. \tag{21}$$

It is the violation of the third condition that leads to the mechanical instability of bcc hard spheres.

For comparison to the literature, it is useful to define two useful quantities that can be determined from the elastic constants. The first is the bulk modulus

$$B \equiv \frac{C_{11} + 2C_{12} + P}{3}. \tag{22}$$

This quantity is simply the inverse isothermal compressibility for the crystal. The second is Poisson's ratio

$$\nu \equiv \frac{C_{12} + P}{C_{11} + C_{12}}. \tag{23}$$

This ratio measures the contraction of the transverse direction in response to a uniaxial stretching. It is this quantity that was predicted incorrectly to be negative by the early density-functional calculations. Using Eq. (21), it can be shown easily that mechanical stability requires

$$\nu < \tfrac{1}{2}. \tag{24}$$

III. WEIGHTED-DENSITY-FUNCTIONAL THEORY

In the canonical ensemble, a density-functional theory (DFT) is a procedure for determining the Helmholtz free energy $\mathscr{F}$ associated with a given spatially dependent single-particle density $\rho(\mathbf{r})$; i.e., $\mathscr{F}$ is determined as a *functional* of $\rho(\mathbf{r})$. The equilibrium free energy and microscopic density can then be found by minimizing this functional $\mathscr{F}(\rho)$ over the space of single-particle densities—subject to the constraint that the volume and total number of particles remains fixed. For a detailed description of basic classical density-functional theory and its mathematical justifications, see the review by Evans.[22]

The functional $\mathscr{F}(\rho)$ can be written as the sum of an ideal part $\mathscr{F}_{id}(\rho)$ and an excess part $\mathscr{F}_{ex}(\rho)$ due to the interparticle interactions

$$\mathscr{F}(\rho) = \mathscr{F}_{id}(\rho) + \mathscr{F}_{ex}(\rho). \tag{25}$$

The ideal part is known exactly and for a monatomic system is given by

$$\mathscr{F}_{id}(\rho) = \int d\mathbf{r}\, \rho(\mathbf{r}) \{ \ln[\Lambda^3 \rho(\mathbf{r})] - 1 \}, \tag{26}$$

where Λ is the thermal wavelength. The excess part is, in general, unknown. Therefore, the central task of a density-functional theory is to provide a suitable approximation scheme for this quantity.

While a variety of methods have been developed for approximating $\mathscr{F}_{ex}$, they can for the most part be divided into two classes. In the first class, originating in the work of Ramakrishnan and Yussouff[15] and Haymet and Oxtoby,[7] the functional for the excess free energy of the inhomogeneous phase is expressed as a functional Taylor series in the single-particle density about some homogeneous reference liquid. The coefficients of the nth-order expansion term are the n-body direct-correlation functions evaluated in the homogeneous phase. As these functions are only readily available for $n \leqslant 2$, the expansion is generally truncated at second order.

In the hope of correcting the deficiencies of the "second-order" DFTs, a new approach was initiated by Tarazona.[8] This weighted density-functional method is a modification of the usual local-density approximation (LDA) for inho-

mogeneous systems. The most successful such theory to date, based on simplicity and accuracy, is the so-called modified weighted-density approximation (MWDA) of Denton and Ashcroft,[13] which is a simplification of the earlier weighted-density approximation (WDA) of Curtin and Ashcroft.[10]

In the MWDA, the excess free energy of the inhomogeneous phase is given by the homogeneous free energy evaluated at a spatially *independent* weighted density

$$\beta \mathscr{F}_{ex}(\rho) = N\beta f_0(\hat{\rho}), \tag{27}$$

where the weighted density is defined by

$$\hat{\rho} = \frac{1}{N} \int d\mathbf{r}_1 \rho(\mathbf{r}_1) \int d\mathbf{r}_2 \rho(\mathbf{r}_2) w(|\mathbf{r}_1 - \mathbf{r}_2|; \hat{\rho}). \tag{28}$$

The weighting function w is determined from requirements that it be normalized to unity and that the resulting free-energy functional yields the correct two-particle direct-correlation function in the homogeneous limit. The resulting equation for the weighting function is easily solved algebraically to give

$$w(|\mathbf{r}_1 - \mathbf{r}_2|; \hat{\rho}) = -\frac{1}{2\beta f_0'(\hat{\rho})} \left[c^{(2)}(|\mathbf{r}_1 - \mathbf{r}_2|; \hat{\rho}) + \frac{\hat{\rho}\beta f_0''}{V} \right]. \tag{29}$$

An alternate derivation of the MWDA, which shows its relation to earlier perturbative approaches, has been given recently by Laird and Kroll.[19] It should be noted that in the present calculations, the real-space integrals in Eq. (28) are evaluated most easily by conversion into a reciprocal-space sum by Fourier transform.

Now that the MWDA Helmholtz free energy as a functional of the single-particle density $\rho(\mathbf{r})$ has been specified, the equilibrium structure and free energy are determined by minimizing this functional with respect to variations in $\rho(\mathbf{r})$ subject to the constraint of constant bulk density. Practical calculations require the parametrization of $\rho(\mathbf{r})$ in order to reduce the minimization dimensionality. All calculations reported in this and earlier calculations were done using a generalized Gaussian parametrization for the solid single-particle density

$$\rho(\mathbf{r}) = \left(\frac{\pi}{|\alpha|} \right)^{3/2} \sum_{\{\mathbf{R}_i\}} \exp[(\mathbf{r} - \mathbf{R}_i) \cdot \alpha \cdot (\mathbf{r} - \mathbf{R}_i)], \tag{30}$$

where α is a matrix containing the Gaussian width parameters and $\{\mathbf{R}_i\}$ represents the set of real-space lattice vectors for the particular solid structure under consideration (e.g., fcc or bcc). This parametrization differs from the usual isotropic Gaussian form often used in density-functional freezing calculations because the calculation of the elastic constants requires distortion of the lattice away from the strict cubic symmetry of the fcc or bcc lattice, therefore requiring an anisotropic description of the crystal density peaks. The number of minimization variables used in the calculation of a particular elastic constant is then dependent on the symmetry of the concomitant lattice distortion. One advantage to the Gaussian parametrization is that the ideal part of the free energy [Eq. (4)] can be evaluated analytically

TABLE I. Thermoelastic constants for the fcc hard-sphere calculated using the MWDA with the Percus–Yevick hard-sphere data.

$\rho\sigma^3$	P	C_{11}	C_{12}	C_{44}	B	C_1	ν
0.90	6.54	24.80	1.77	21.09	11.63	4.97	0.313
0.92	6.84	30.55	4.56	23.66	15.50	6.15	0.325
0.94	7.21	36.06	6.65	26.37	18.86	7.49	0.325
0.96	7.64	41.60	8.75	29.54	22.25	8.78	0.326
0.98	8.14	47.75	10.88	33.17	25.88	10.3	0.324
1.00	8.70	54.65	24.20	37.34	29.92	12.0	0.323
1.02	9.34	62.53	15.82	42.16	34.50	14.0	0.321
1.04	10.06	71.51	18.92	47.82	39.80	16.2	0.320
1.06	10.88	82.32	22.42	54.47	46.01	19.1	0.318
1.08	11.80	94.98	26.68	62.44	53.38	22.4	0.316
1.10	12.86	110.15	31.88	71.69	62.26	26.3	0.315
1.12	14.08	128.57	38.25	83.20	73.05	31.1	0.314
1.14	15.48	151.24	46.20	97.11	86.37	37.0	0.312
1.16	17.12	179.58	56.27	114.5	103.1	44.5	0.311
1.18	18.07	215.6	69.3	136.9	124.4	54.1	0.310
1.20	21.34	261.7	86.7	165.2	152.2	66.1	0.310
1.225	24.98	343.4	116.6	214.1	200.5	88.4	0.308
1.25	29.70	464	162.6	286.2	273.0	121	0.307
1.275	36.17	658	232	402	386.1	147	0.301

TABLE II. Thermoelastic constants for the bcc hard-sphere solid calculated using the MWDA with the Percus–Yevick hard-sphere data.

$\rho\sigma^3$	P*	C_{11}	C_{12}	C_{44}	B	C_1	ν
0.92	8.67	16.3	−6.0	25.1	4.30	2.48	0.258
0.94	9.04	26.1	14.1	30.3	24.4	1.97	0.435
0.96	9.65	44.9	22.3	35.3	33.5	1.32	0.481
0.98	10.43	53.3	31.5	41.4	42.2	0.49	0.494
1.00	11.38	62.7	41.2	48.7	52.2	−0.60	0.51
1.02	12.53	74.0	53.1	56.7	64.2	−2.06	0.52
1.04	13.92	87.9	68.2	66.0	79.4	−4.05	0.53
1.06	15.60	105.4	87.8	72.4	98.9	−6.80	0.54
1.08	17.68	127.6	113.7	54	124	−10.6	0.54
1.085	18.27	···	···	36	···	···	···
1.10	20.24	154.0	146.5		156	−16.5	0.56
1.12	23.3	179	181		188	−26	0.57
1.14	26.9	195	215		217	−37	0.59
1.16	31.2	258	280		283	−61	0.58
1.18	37.0	377	398		403	−47	0.56
1.20	45.3	576	596		604	−56	0.55

$$\beta F_{\mathrm{id}}(\alpha) = \frac{3}{2}\ln\left(\frac{|\alpha|}{\pi}\right) + 3\ln(\Lambda) - \frac{5}{2}. \tag{31}$$

The validity of the Gaussian approximation is discussed in detail in Ref. 12.

IV. RESULTS AND DISCUSSION

Implementation of the MWDA for the calculation of the elastic constants for hard-sphere crystals requires as input the thermodynamics and structure of the hard-sphere fluid over a range of densities. Fortunately, for the hard-sphere system, these input data are available in relatively accurate, analytical form from the exact solution of the Per-

cus–Yevick equation derived independently by Werteim[23] and Thiele.[24] Since the weighted densities produced within the MWDA are considerably lower than the bulk densities of the solids studied, the Percus–Yevick approximation for hard spheres should be adequate for this calculation as it breaks down only at high densities near freezing.

Using Eqs. (12)–(18), the elastic constants for the fcc and bcc hard-sphere crystals have been calculated. A five-point finite difference formula to evaluate the requisite derivatives with $\delta\epsilon$ ranging from 0.001 to 0.1. For the fcc system, the calculated values of the pressure P and the elastic constants C_{11}, C_{12}, and C_{44} are given in Table I and plotted in Fig. 1. Also in Table I are shown the derived quantities B and ν. With the exception of the dimensionless ratio ν, all quantities are in units of $(k_B T)/\sigma^3$, where k_B is Boltzmann's constant, T is the temperature, and σ is the hard-sphere diame-
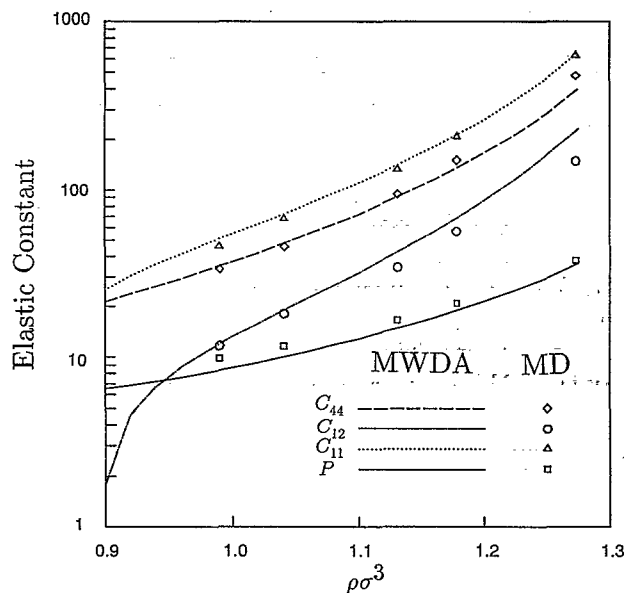

FIG. 1. The pressure and elastic constants for the hard-sphere fcc crystal as functions of density. All quantities are in units of $(k_B T)/\sigma^3$. The lines are the MWDA density-functional results and the symbols represent those of the computer simulations (Ref. 16).
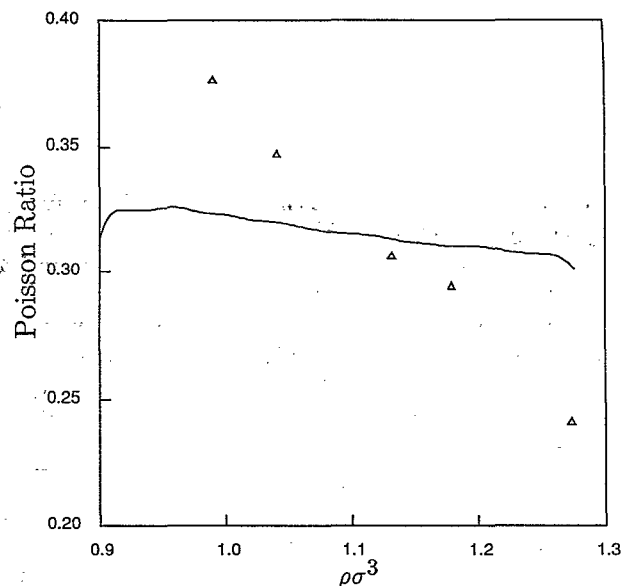

FIG. 2. The Poisson ratio for the fcc crystal. The solid line gives the MWDA theoretical results and the circles are from the simulations (Ref. 16).
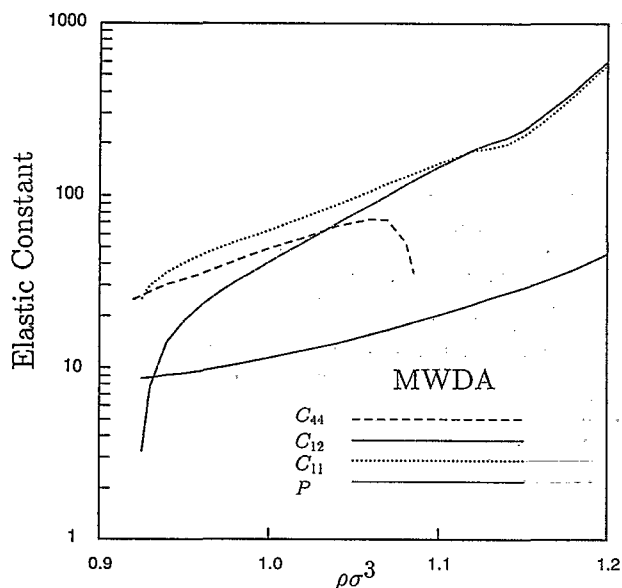
FIG. 3. The MWDA pressure and elastic constants for the hard-sphere bcc crystal as functions of density. All quantities are in units of $(k_B T)/\sigma^3$.

FIG. 4. The MWDA elastic constant $C_\perp$ in units of $(k_B T)/\sigma^3$ [see Eq. (21)] for the bcc (dotted line) and fcc (solid line) crystals. The simulation values (Ref. 16) for the fcc crystal are also shown (circles).

ter. The computer simulation results[16] are also plotted in Fig. 1 and one can see that the agreement is excellent. Please note that the scale is logarithmic. This was done so that all the data could be displayed conveniently on one graph. The greatest error occurs for C_{12}, which is about a factor of 1.5 too large at the highest densities calculated. These results for the MWDA represent a significant improvement over those of earlier density-functional calculations.

The calculated values for the Poisson ratio ν for the fcc crystal are plotted in Fig. 2 together with the simulation values. While both show a negative slope as a function of density, the trend is more pronounced in the simulations. This is due primarily to the overestimation by the theory of the value of C_{12} at high density. Note that for all densities, the Poisson ratio is positive in agreement with the simulations and in contrast to the early "second-order" density-functional calculations.

Table II contains the same information as in Table I for the bcc hard-sphere crystal. The bcc pressure and the elastic constants are plotted in Fig. 3. The maximum calculated density for the bcc crystal is lower than that of the fcc calculation because, since the maximum packing fraction of bcc is lower than that of fcc, the bcc elastic constant becomes large at lower densities than those for fcc.

The question of the stability of the bcc hard-sphere crystal is answered by evaluating the elastic constant $C_\perp$ defined in Eq. (21). The physical distortion represented by $C_\perp$ is a *contraction* along one Cartesian direction (e.g., x) coupled with a simultaneous *expansion* along a perpendicular direction (e.g., y). Mechanical stability requires that this quantity be positive. For both the fcc and bcc crystals, $C_\perp$ is shown in Fig. 4. As expected, this quantity is positive at all densities for the fcc solid. For the bcc solid, $C_\perp$ is small and positive for reduced densities below about 1.0 and negative above. This would indicate that the bcc solid is stable at densities (below 1.0) and unstable at high densities. This somewhat curious
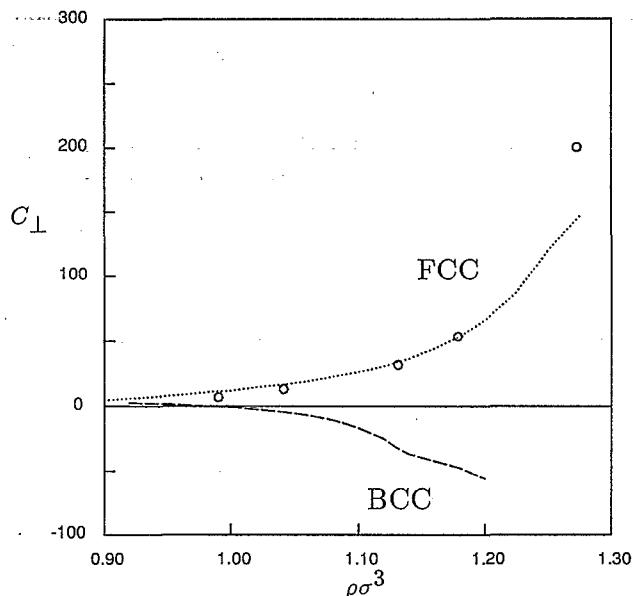
result has also been seen by McCarley and Ashcroft[25] in their recent MWDA study of bcc hard-sphere stability. The densities at which the bcc crystal is predicted to be mechanically stable are well below the lowest thermodynamically stable solid density. This low-density stability is counterintuitive and is most certainly an artifact of the theory caused by the anomalous drop in C_{12} at low densities for the bcc (and to a smaller extent the fcc) crystal.

A curious and unforeseen trend in the bcc elastic constants is the sudden drop in C_{44} at a reduced density of about 1.09, indicating the onset of yet another form of mechanical shear instability [see Eq. (20)]. Above $\rho\sigma^3 = 1.085$, this quantity actually goes negative. Analysis of the free energy as a function of ϵ_3 [using the displacement tensor $u_{ij}^{(3)}$ defined in Eq. (14)] shows that this drop is due to the transformation of the minimum at $\epsilon_3 = 0$ (the undistorted crystal) into a saddle point.

In summary, the modified weighted-density approximation of Denton and Ashcroft has been shown to give results for the fcc hard-sphere elastic constants that are superior to those calculated previously using other density-functional approaches. Given the extreme sensitivity of the calculated elastic constants on the density-functional method used, this is a very important result. In addition, except at low densities below the usual region of interest for hard-sphere crystals, the bcc hard sphere is predicted correctly by the MWDA to be unstable to shear. This is further evidence that this unstable phase is well described by such methods and could be used as a starting point for perturbation theory studies of stable bcc phases in systems with longer-ranged potentials.

ACKNOWLEDGMENTS

[1] T. V. Ramakrishnan, Pramara **22**, 365 (1984).

[2] G. L. Jones, Mol. Phys. **61**, 455 (1986).

[3] M. V. Jarić and U. Mohanty, Phys. Rev. Lett. **58**, 230 (1987); Phys. Rev. B **37**, 4441 (1988).

[4] E. Velasco and P. Tarazona, Phys. Rev. A **36**, 979 (1987).

[5] M. Baus and H. Xu, Phys. Rev. A **38**, 4348 (1988).

[6] W. G. Hoover and F. M. Ree, J. Chem. Phys. **49**, 3609 (1968).

[7] A. D. J. Haymet and D. Oxtoby, J. Chem. Phys. **74**, 2559 (1981).

[8] P. Tarazona, Mol. Phys. **52**, 81 (1984).

[9] G. L. Jones and U. Mohanty, Mol. Phys. **54**, 1241 (1985).

[10] W. A. Curtin and N. W. Ashcroft, Phys. Rev. A **32**, 2909 (1985).

[11] J. L. Colot, M. Baus, and H. Xu, Mol. Phys. **57**, 809 (1986).

[12] B. B. Laird, J. D. McCoy, and A. D. J. Haymet, J. Chem. Phys. **87**, 5449 (1987).

[13] A. R. Denton and N. W. Ashcroft, Phys. Rev. A **39**, 4701 (1989).

[14] J. F. Ludsko and M. Baus, Phys. Rev. Lett. **64**, 761 (1990).

[15] T. V. Ramakrishnan and M. Yussouff, Phys. Rev. B **19**, 2775 (1979).

[16] D. Frenkel and A. J. C. Ladd, Phys. Rev. Lett. **59**, 1169 (1987).

[17] K. J. Runge and G. V. Chester, Phys. Rev. A **36**, 4852 (1987).

[18] W. A. Curtin and K. J. Runge, Phys. Rev. A **35**, 4755 (1987).

[19] B. B. Laird and D. M. Kroll, Phys. Rev. A **42**, 4810 (1990).

[20] B. B. Laird and A. D. J. Haymet, Mol. Phys. **75**, 71 (1992).

[21] D. C. Wallace, in *Solid State Physics*, edited by H. Ehrenreich, F. Seitz, and D. Turnbull (Academic, New York, 1970), Vol. 25, p. 301.

[22] R. Evans, Adv. Phys. **28**, 143 (1979).

[23] M. S. Wertheim, Phys. Rev. Lett. **10**, 321 (1963).

[24] E. Thiele, J. Chem. Phys. **39**, 474 (1963).

[25] N. W. Ashcroft and J. S. McCarley (private communication).